Wall Heat Fluxes at Different Oxidizer to Fuel Ratios in Rocket Combustion Chamber with Porous Injector Head

Victor P. Zhukov and Dmitry I. Suslov
Institute of Space Propulsion, German Aerospace Center (DLR)
Langer Grund, 74239 Hardthausen, Germany

Abstract

Rocket combustion chamber with porous injector head, which is a new concept for injecting propellants, is considered in this work. The sub-scale combustion chamber with the porous injector head fuelled by cryogenic oxygen and hydrogen has been tested. The hot tests have been performed at pressure of 80 bar and the mass ratios of oxidizer to fuel of 6, 5, and 1.5. Pressures, wall temperatures, and wall heat fluxes have been measured along the axis of the chamber during the hot tests. The wall heat fluxes have been measured by the calorimetric method. To analyse the experimental data numerical simulations are performed using the commercial CFD code ANSYS CFX. The turbulent flow is modelled by the Favre averaged Navier–Stokes equations and the Shear-Stress-Transport model. The turbulent combustion is modelled using the modified Eddy Dissipation Model (EDM). The comparison of the simulation results with the experimental data shows the good agreement of the modified EDM model with the experiment. The agreement of the model with the experiment is achieved by applying additional parameters which are dependent on the local mixture composition: "Flame Temperature", "Chemical Timescale", and "Mixing Rate Limit".

1. Introduction

The application of porous materials can improve the performance of rocket combustion chambers used now. A porous injector head can provide effective mixing of fuel and oxidizer at low pressure drop in the injector head. This new injection concept is being under development at the German Aerospace Center (DLR-Lampoldshausen) [1-3]. Nowadays, the porous injector faceplates are used in some rocket engines (for example: SSME and J-2) where the small fraction of the fuel flow is fed through the porous injector faceplate in order to cool it and the main part of the fuel is still injected through coaxial injectors [4]. Coaxial injectors proved their efficiency, but they require a very precise manufacture and keep their efficiency in the narrow range of mass flows which is bounded from above and below. These problems can be easily solved by the application of a porous injector head. According to the hot-tests at DLR-Lampoldshausen [2] the porous injector head (Fig. 1) allows to maintain the high combustion efficiency over the wide throttling range from 37.5% to 125%. Besides the manufacture costs and the throttling capability porous injector head has two additional advantages over conventional coaxial injectors. Porous injector head operates at a smaller pressure drop than injector heads with coaxial injectors. The small diameter of the injectors in a porous head results in a small jet break-up distance which allows reducing chamber length. Such features improve the performance of rocket engines.

Rocket combustion chambers are exposed to severe thermal loads during the burn. The components of a thrust chamber assembly (injector head, side walls, and nozzle) require the adequate cooling. The proper design of a rocket combustion chamber needs the knowledge of the heat fluxes inside the chamber. The accumulated experience (experimental tests and simulations) with the conventional impinging and co-axial injectors is sufficient for combustion chamber design; however the existed knowledge on porous injector heads is not enough.

Zhukov and Haidn [5] considered the heat transfer in a porous injector plate at the conditions of the present work. They found an analytical expression connecting the incident heat flux and the temperature of the hot side wall of a porous injector head. It was shown that the heat loads are not problematic at least for an injector head made from sintered bronze (i.e. for the injector head which is used in the present work). However, the thermal loads are still an issue for other parts of thrust chamber assembly: side walls and nozzle.

While the wall heat flux reaches a maximum in the throat of the combustion chamber, the peculiarities of the injector head should be negligible there and further downstream in the divergent nozzle (the flow in a "good" combustion chamber should be already uniform upstream the throat). The particularities of the porous injector head should come out at the first 100 mm from the injector plate. At this location the parameters of the flow depend strongly on the

injection conditions. The flow and the heat fluxes in a combustion chamber with coaxial injectors were studied by many other researchers, e.g., in the extensive series of works from Airbus D&S [6-8]. However, the numerical analysis of the flame of porous injector head has not been done yet.
In the present work the incident heat fluxes to the side walls of the combustion chamber with a porous injector head are studied both experimentally and theoretically. In our previous work [3] we already simulated the flow in the combustion chamber with porous injector head, however it gave us only preliminary results which showed the direction of the further development of numerical modelling.

2. Experiments

Segmented, water cooled combustion chamber model "B" and porous injector head API-68 (Fig. 1) were designed, manufactured and tested at DLR-Lampoldshausen. The combustion chamber operates with LOx/H_2 or LOx/CH_4 propellant combination in the wide pressure range up to 12 MPa. The hot tests have been done at the European Research and Technology Test Facility P8. This test facility operates in a controlled blow-down mode and enables investigations with liquid and gaseous hydrogen at typical rocket engine operating conditions.
The segmented design enables the implementation of various test equipment without additional expenditures. The combustion chamber has an inner diameter of 50 mm and consists of six cylindrical elements, each of 50 mm length, with a separate cooling supply. The heat exchange occurs in a row of cylindrical cooling channels. Two collectors in each section provide a uniform mass flow through all cooling channels. The changeable nozzle section allows changing the contraction ratio ($A_{comb.chamber}/A_{throat}$) from 2 to 8.4. The nozzle segment with a 28 mm throat and the corresponding contraction ratio of 3.2 has been used in the present study.
Combustion chamber "B" is used predominantly to study the heat transfer on the hot-side wall and the influence of different design solutions (for example, a new injector head design) on the thermal loads on the combustion chamber walls. Only the calorimetric measurement method has been used in the current study. The wall heat fluxes have been determined using measurements of temperature and pressure at the inlet and the outlet of each section according to the formula:

$$Q = \varphi \cdot [h_{out}(T_{out},P_{out}) - h_{in}(T_{in},P_{in})], \quad \textbf{(1)}$$

where Q – heat flux to the segment, φ – coolant mass flow rate, $h_{out}(T_{out},P_{out})$ – specific enthalpy of water at the outlet of a cylindrical segment as the function of temperature and pressure, $h_{in}(T_{in},P_{in})$ – specific enthalpy of water at the inlet of a segment. An additional temperature sensor measures the surface temperature on the hot-gas side.

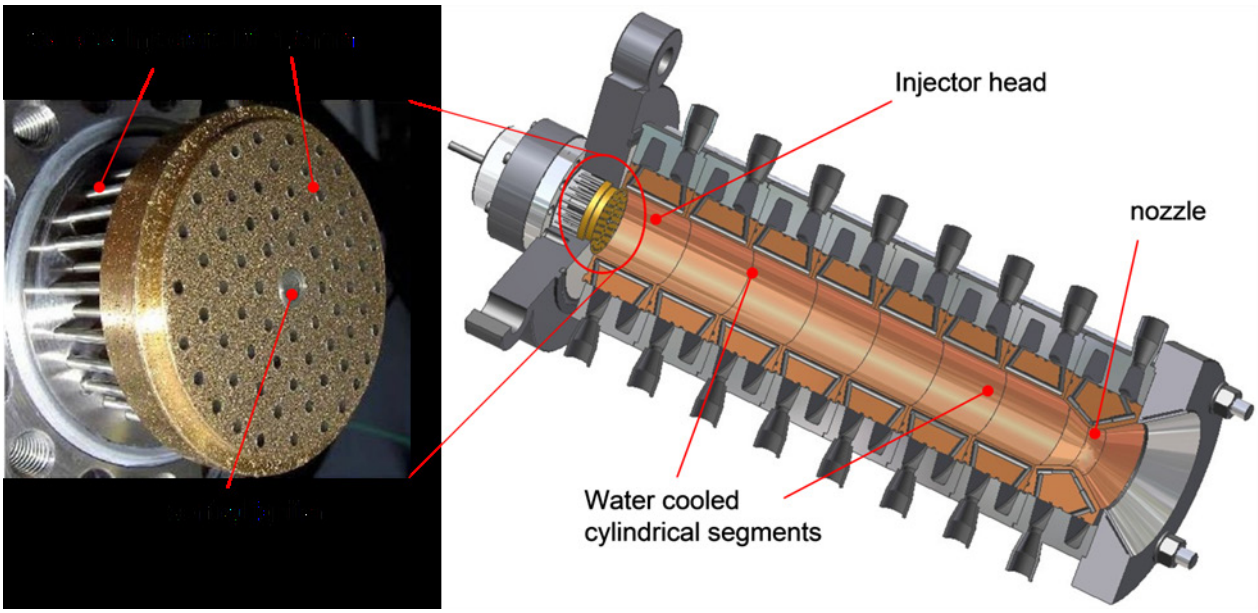

Figure 1: The photo of porous injector head API-68 and the cross-section of sub-scale combustion chamber model "B".

Table 1: Conditions of the hot run tests

ROF	6	5	1.5
Mass flow rate, O_2	1.808 kg/s	1.704 kg/s	1.241 kg/s
Temperature, O_2	120 K	120 K	120 K
Mass flow rate, H_2	0.299 kg/s	0.337 kg/s	0.813 kg/s
Temperature, H_2	60 K	60 K	50 K
Pressure in combustion chamber at x = 0 mm	79.4 bar	79.1 bar	78.5 bar

Table 2: Experimental results: wall temperatures and wall heat fluxes

Segment	Distance to injector head	ROF 6		ROF 5		ROF 1.5	
		T_{wall}	Q_{wall}	T_{wall}	Q_{wall}	T_{wall}	Q_{wall}
S1	0–50 mm	357 K	0.78 MW/m^2	341 K	0.66 MW/m^2	306 K	-1.59 MW/m^2
S2	50–100 mm	458 K	33.5 MW/m^2	444 K	30.3 MW/m^2	365 K	14.9 MW/m^2
S3	100–150 mm	552 K	29.6 MW/m^2	531 K	26.6 MW/m^2	411 K	11.6 MW/m^2
S4	150–200 mm	644 K	29.4 MW/m^2	618 K	27.1 MW/m^2	463 K	14.4 MW/m^2
S5	200–250 mm	559 K	25.1 MW/m^2	544 K	23.3 MW/m^2	433 K	11.8 MW/m^2
S6	250–300 mm	647 K	32.3MW/m^2	627 K	30.2 MW/m^2	478 K	17.0 MW/m^2
Nozzle	300–355 mm	629 K	38.3 MW/m^2	603 K	35.8 MW/m^2	444 K	19.8 MW/m^2

The key feature of the tested combustion chamber is the porous injector head called API-68 (Advanced Porous Injector, 68 injectors), see Fig. 1. The injector plate is made from sintered bronze. Hydrogen is fed into the combustion chamber through the massive porous plate which consists of sintered bronze beads with a diameter of ~0.6 mm. Liquid oxygen is injected through 68 separate injectors distributed uniformly over the porous plate. A single injector is a cylindrical tube with an inner diameter of 1.5 mm. The thickness of the injector tip amounts only 0.25 mm, and fuel and oxidizer get in direct contact immediately after the injection in contrast to classical showerhead injector heads, which looks similar at first sight. In the centre of the injector plate the outlet of an igniter torch is located. The simplicity of the used design offers a large potential for manufacturing cost savings.
The combustion chamber with API-68 shows a stable behaviour with the pressure drop between the fuel dome and the chamber below 5% of the mean chamber pressure. The experimental conditions are given in Tables 1; the results of the hot test are presented in Table 2.

3. Simulations

The simulations have been performed using the commercial CFD code ANSYS CFX [9], which utilizes the finite volume element method (FVEM). The numerical simulations of the flow inside the chamber have been carried out in a three-dimensional computational domain, which represents one-eighth of the chamber. The domain includes the combustion chamber, oxygen injectors, and the nozzle, see Fig. 2. In the numerical domain the turbulent flow of a compressible reactive fluid has been simulated. The simulations have been performed on a Dell PowerEdge R815 server computer with 48 cores.
There are many examples where the flow inside the rocket combustion chamber is simulated in a two-dimensional axisymmetric domain (even in the case of the injector head with multiple injectors), for example [7,8]. The substitution of the real geometry by the 2D geometry enables the significant reduction of the computational power which is required for the simulation. Preliminary study [3] showed that in the current case the modelling in 2D domain gives acceptable but not the very accurate results, that the use of the coarse 3D numerical mesh gives better results than the use of the very fine 2D mesh. The heat flux to the wall is very sensitive to the arrangement of the

injectors nearest to the wall. (This is also supported by the longstanding experimental experience at our institute.) The semi-rectangular pattern of injectors of the tested injector head API-68 cannot be represented adequately in a 2D axisymmetric geometry. That is why in spite of the significant increase of the size in the numerical mesh the 3D numerical domain has been employed. The arrangement of the injectors has a 90^0 rotational symmetry plus a reflective symmetry diagonally (Fig. 1), so the geometry of the injector head and the combustion chamber can be fully represented by the sector of 45^0, see Fig. 2.

The simulations were performed on a tetrahedral unstructured mesh with prismatic layers near the walls. The numerical mesh was generated using the computer program ICEM from the package ANSYS CFD. Around twenty different meshes were tested until the final mesh, which gives the mesh independent solution and has a reasonable amount of nodes (12 Mio nodes), has been found. The mesh is refined near the side walls, the injector posts, and the axes of the injectors at the first 50 millimetres from the injector head. The spacing between the nodes varies from 4 μm to 4 mm (the most coarsened mesh is located in the diverging part of the nozzle). The expansion ratio was globally set to 1.15.

The flow in the combustion chamber has been modelled as the stationary solution of the Favre averaged Navier–Stokes equations. The turbulence has been modelled with the help of the Shear-Stress-Transport (SST) model using the standard values of the coefficients and the "automatic" wall function [10]. The transport in turbulent flow has been modelled with the turbulent Schmidt number of 0.7 (The value of 0.7 is recommended for high-Reynolds-number jet flows by Yimer et al. [11]). The turbulent Prandtl number has been set to the value of 0.9, which is a value by default.

The simulations have been performed using the modified Eddy Dissipation Model. In the model the chemical transformations occurs by global reaction

$$½H_2 + O_2 = (1\text{-}y)H_2O + y\cdot X, \qquad \textbf{(2)}$$

where X corresponds to other products and depends on additional model parameters. The used combustion model use the assumption of a thin flame: chemical reactions are infinite fast, and chemical transformations are limited by turbulent mixing. Hence,

$$\text{rate} \sim \varepsilon/k, \qquad \textbf{(3)}$$

where ε is the turbulence eddy dissipation, and k is the turbulent kinetic energy.

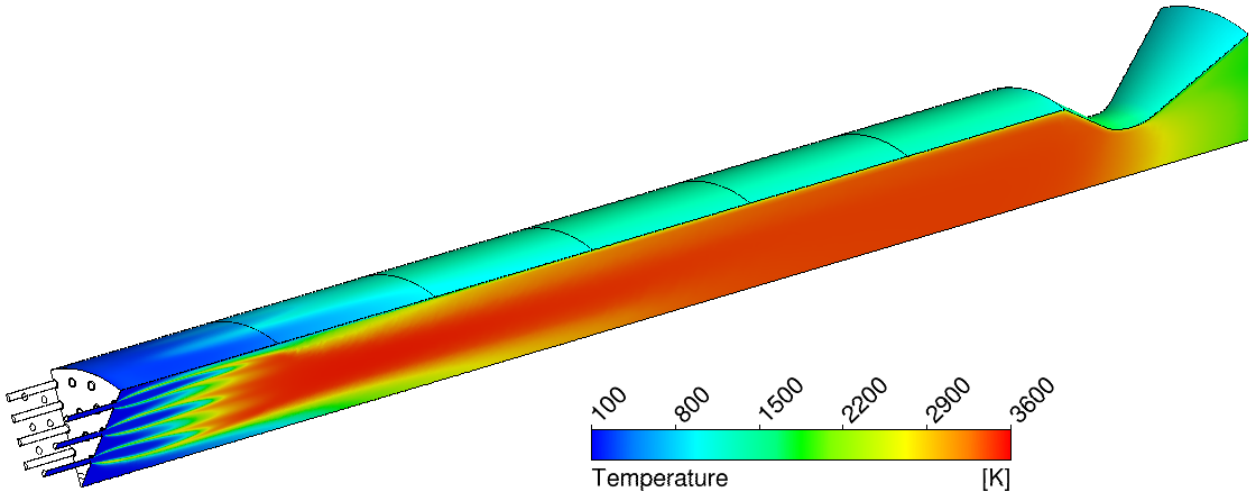

Figure 2: Simulated temperature field at the symmetry plane and at the walls of the combustion chamber.

The advantages of the Eddy Dissipation Model (EDM) are the simplicity and the robustness, but to achieve the acceptable results the model should be extended, especially in the case of rocket combustion (reaction of pure fuel and oxygen at high pressures). At high temperatures (>3000 K) the dissociation of H_2O starts to play a role, in other words (1-y) in Eq. (2) is notably less than 1. To obtain the correct flame temperature in the combustion chamber, which is very important for the heat balance of the combustion chamber and the predictions of the heat fluxes, an additional parameter (called "Flame Temperature") was introduced in the model. The reaction rate is set to zero when the temperature of the reactive mixture reaches the value of the "Flame Temperature" which is precalculated by the use of the program NASA CEA [13]. Another important additional parameter in the model is the "Extinction

Temperature". The propellants are injected into the chamber at very low temperature, so it is necessary to set the reaction rate to zero when the temperature of the reactants is obviously below the flammability limit. Here, in contrast to the standard formulation of the EDM model in CFX, the parameters: "Flame Temperature", "Chemical Timescale", and "Extinction Temperature" are not constant, but the functions of mixture fraction, which is the mass fraction of element hydrogen in mixture.
In the combustion chamber the temperatures vary from 100 to 3650 K, and the pressure is high. Therefore, the modelling of the thermodynamic properties of the gas mixture in the combustion chamber is not a simple task. All three major components of the mixture (H_2, O_2, and H_2O) have significant distinctions from ideal gas. Three main non-ideal phenomena have been taken into account: the transition from ortho to para state for hydrogen at low temperatures, the real gas behaviour of oxygen at the low injection temperature, and the dissociation of water at high temperatures. The components of the mixture obey the Peng–Robinson real gas equation of state in the model. The enthalpy and the entropy of the components have been defined using NASA polynomials [14]. The dynamic viscosity and the thermal conductivity of the mixture and its components have been defined using the empirical formulas according to the recommendations of White [15]. The diffusion coefficients have estimated using the data from Kikoin [16]. The viscosity, the thermal conductivity, and the diffusivity of gases grow with temperature, and the model takes this effect into account. CFX defines the property of multicomponent mixture using mass averaging, which leads to the wrong estimation of the transport coefficients for the mixture of hydrogen with oxygen [17]. For this reason, the transport properties of the gas mixture have been modelled separately using the CFX Expression Language. From the original CFX models only the turbulence model and the equation of state were left without modification.

4. Results and discussion

The general idea about the flow in the combustion chamber is given in Fig. 2. The flow in the combustion chamber is characterized by a pressure drop and the simultaneous increase of the wall heat flux within the first 50 mm from the injector face, Fig. 3 and 4. This occurs due to the short length of oxygen jets. Breakup length is connected with injector diameter, namely, an injector with a smaller diameter is characterised by a smaller breakup length. As one can see, the numerical models capture the behaviour of the flow, and moreover the modified EDM model gives the results which agree with the experimental data within experimental error.

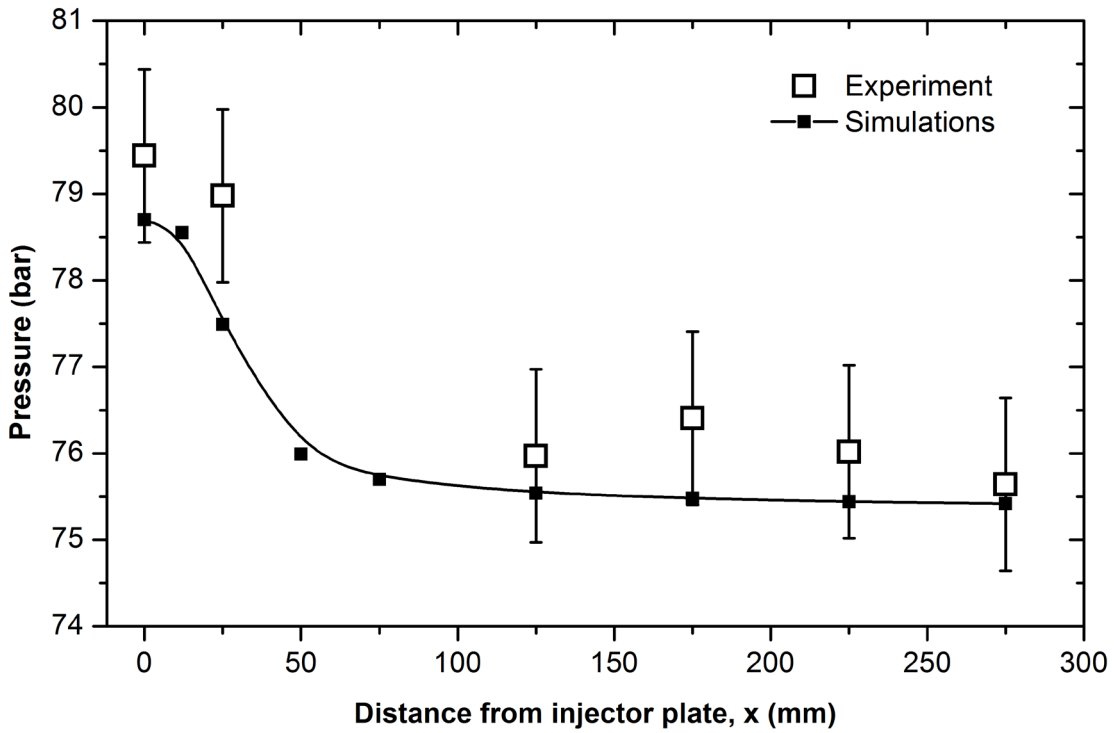

Figure 3: Pressure profile in the combustion chamber: experimental data and simulation results.

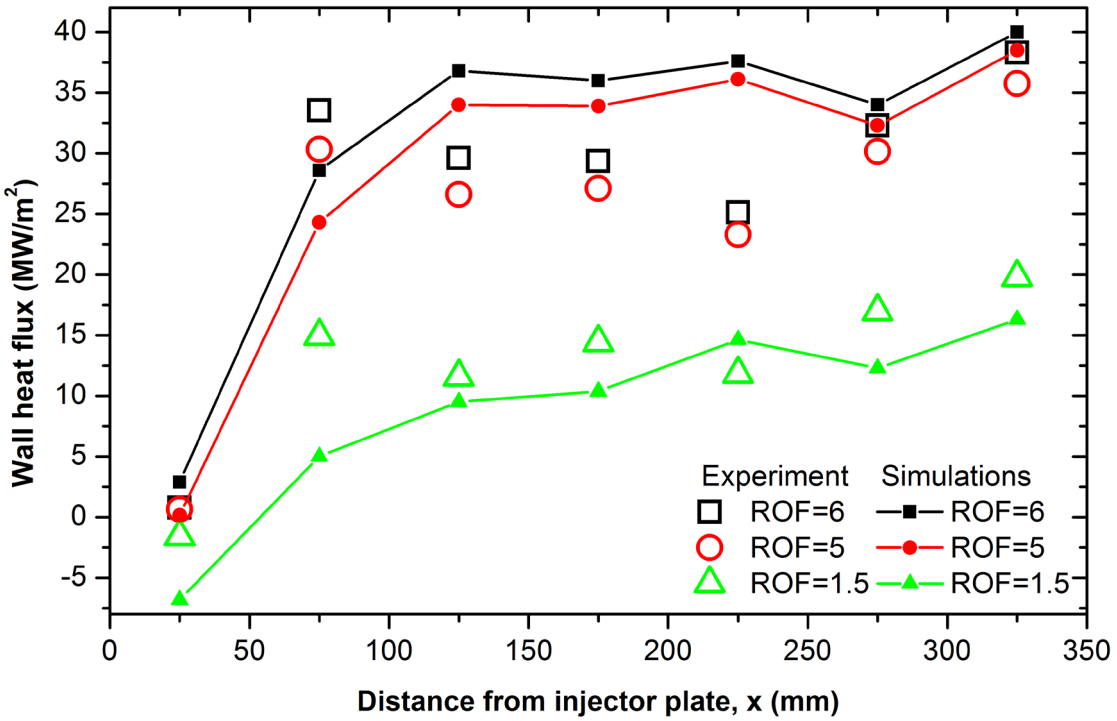

Figure 4: Comparison of the measured and predicted wall heat fluxes. Open symbols – experiment; lines and solid symbols – simulations.

The wall heat flux in the experiment and in the simulations has slightly different behaviour. In the experiment the wall heat flux has a maximum in the second section. This distinguishes the combustion chambers with porous injector heads from the combustion chambers with coaxial injectors where the wall heat flux gradually increases towards to the nozzle [6-8]. However, the numerical model predicts the high wall heat flux in the third, fourth, and fifth calorimetric sections. The most problematic locations for the used CFD model are the second and fifth sections where the model predicts the wall heat fluxes which are different from the measured values, namely, the clearly lower wall heat flux in the second section and the clearly higher heat flux in the fifth section.
The modified EDM model accurately predicts the wall heat flux (and temperature) in the throat, see Fig. 4. In the throat the gas expands and the temperature decreases. As soon as the temperature in the throat falls below the “Flame Temperature”, the reaction occurs again. This slightly compensates the temperature drop in the throat. The flame temperature is determined by the equilibrium between H_2O and OH. When the temperature of the products decreases, the equilibrium shifts towards the formation of H_2O. Thus, the behaviour of the modified EDM model is very close to the real behaviour of the flow in the throat section.
The main benefit of the modified EDM model is the simplicity, and the fact that the parameters of the EDM model have a clear physical meaning. In spite of the apparent crudity of the EDM model, it is not primitive. By the modified EDM model flame is characterized by six parameters in CFX. Three of them have been set as the functions of the local mixture composition here. Hence, the total amount of the coefficients in the used EDM model corresponds to a reaction mechanism with approximately four–six reactions.

5. Conclusions

The wall heat fluxes in the combustion chamber with porous injector head API-68 have been measured by the calorimetric method at pressure of 80 bar and ratio-to-fuel ratios of 6, 5 and 1.5. The experimental results are characterised by a pressure drop and the simultaneous increase of the wall heat flux within the first 50 mm which has been explained by the effect of the small injector diameter.
The flow inside the combustion chamber has been simulated using the SST turbulence model and the modified EDM combustion model. The numerical model predicts the pressures inside the combustion chamber within the experimental error. The CFD model gives the adequate prediction of the wall heat flux. However, the used model needs the further development, verification, and validation. The CFD solution has been obtained on a mesh with

12 Mio nodes. The numerical parameters indicate that the used mesh is still not fine enough. Thus, the next step in the development of the present model will be the mesh convergence study.

Acknowledgments

The authors are grateful to Christian Fromm at the German Aerospace Center (DLR-Lampoldshausen) for valuable comments that improved the paper.

References

[1] Lux, J., D. Suslov, and O. J. Haidn. 2007. Aerosp. Sci. Technol., Vol. 12, pp. 469–477.
[2] Deeken, J., D. Suslov, O. J. Haidn, and S. Schlechtriem. 2011. Combustion Efficiency Sensitivity Studies of the API Injector Concept. In: *49th Aerospace Sciences Meeting including the New Horizons Forum and Aerospace Exposition*. AIAA 2011-0793, Orlando, Florida USA.
[3] Zhukov, V.P., D. I. Suslov, and O. J. Haidn. 2011. CFD Simulation of Flow in Combustion Chamber with Porous Injector Head and Transpirationally Cooled Walls. Paper id: 29 at 4th European Conference for Aerospace Sciences, Saint Petersburg, Russia.
[4] Sutton, G.C. Rocket Propulsion Elements. John Wiley&Sons, 1986/1992/2000.
[5] Zhukov, V.P., and O. J. Haidn. 2013. Proc. Inst. Mech. Eng. G J. Aerosp. Eng. 227 (5) 873–881.
[6] Knab, O., and D. Preclik. 2006. Test case RCM-3: EADS-ST subscale chamber. In: *3rd International Workshop Rocket Combustion Modeling*. Vernon, France, SNECMA, Villaroche.
[7] Mewes, B., J. Görgen, O. Knab, and M. Frey. 2006. Simulation of the EADS-ST subscale chamber using a dense gas approach. In: *3rd International Workshop Rocket Combustion Modeling*. Vernon, France, SNECMA, Villaroche.
[8] Ivančić, B., H. Riedmann, and M. Frey. 2012. Validation of Turbulent Combustion Models for 3D-Simulations of Liquid H2/O2 Rocket Combustors. Proceedings of the International Conference on Space propulsion, Bordeaux, France.
[9] CFX, Software Package. 2009. Version 12.1, ANSYS Germany.
[10] Menter, F.R. 1994. AIAA J., 32 (8) 1598–1605.
[11] Yimer, I., I. Campbell, and L.-Y. Jiang. 2002. Canadian Aeronautics and Space Journal, 48 (3) (2002) 195–200.
[12] Magnussen, B. F., and B. H. Hjertager, 1976. Proc. Combust. Inst. 16, 719–729.
[13] Gordon, S., and B. J. McBride. 1996. Computer Program for Calculation of Complex Chemical Equilibrium Compositions and Applications. NASA Reference Publication 1311.
[14] Burcat, A. 2001. Third Millennium Ideal Gas and Condensed Phase Thermochemical Database for Combustion. Technion Aerospace Engineering (TAE) Report #867, Haifa, Israel.
[15] White, F.M. 1991. Viscous Fluid Flow. McGraw-Hill, New York.
[16] Kikoin., I.1976. Tables of physical values. Atomizdat, Moscow.
[17] Zhukov, V.P. 2012. ISRN Mechanical Engineering, vol. 2012, Article ID 475607, 11 pages. doi:10.5402/2012/475607